REMARKS

This submission is in response to the Office Action dated March 18, 2003.

Claims 1, 3, 4 and 6-25 are pending.

Claims 1, 3, 4 and 6-25 stand rejected over the combination of Barry, U.S. 4,093,235 in view of Moore, U.S. 3,642,281.

Main claim 1 and other claims have been amended to clarify the language. Claim 1 also has been amended to set forth that the gripping wing spaced from the end of the elongated parallelepiped body of the multi-token is within the outer periphery of the body.

As set forth in claim 1, the multi-token has the following features:

a.   it is an elongated parallelepiped body. The Examiner's reference to a pyramid shape (Action, page 2, line 14) is therefore irrelevant. The elongated parallelepiped feature permits easy stacking of the multi-tokens. The tokens of the (applicant's) prior Barry patent are in the physical form of an object and cannot be stacked;

b.   a visual representation of the various modes of transportation (air, boat, auto) are placed on at least three of the elongated flat sides of the token body. This makes production of the game less expensive since different shapes of tokens are not required. The transportation mode can be painted on a side of the parallelepiped body or a decal or paper placed thereon;

c.   there is a gripping wing at each of the ends of the elongated parallelepiped body. The gripping wing is <u>spaced</u> from the end of the parallelepiped body and leaves a <u>recess</u>. The purpose of the gripping wing is to improve the tactile feel of the

token in two respects. First, a fingernail can be inserted into the recess to move the token. Second, the flesh of the fingertip that falls into the recess between the wing and the body and encounters the ridge surface and the fingernail that falls into the recess produces a different force pattern on the fingertip and a firmer grip of the token. Reference is made to the two articles by Stephen Mascara and H. Harry Asada entitled *Understanding of Fingernail-Bone Interaction and Fingertip Hemodynamics for Fingernail Sensor Design* and *Finger Posture and Shear Force Measurement using Fingernail Sensor: Initial Experimentation*, attached as Exhibits A and B. These demonstrate, for example, see Section 2.2 of Exhibit B, that any flexing or bending of the fingertip produces a different force pattern. This enhances the tactile "feel" of the fingertip engaging the end of the token and provides a better gripping surface. Also, the fingernails can be inserted into the recess between the token body and the gripping wing to manipulate the token.

The claim also recites that the gripping wing is within the outer periphery of the body. Therefore, the gripping wings do not interfere with the stacking of the multi-token.

      d.   the ends of the multi-token each have a visual indication of the movement status of the tokens, i.e., the GO-NO GO indication as set forth in claims 22-23 and 26-27. This feature interacts with the gameboard.

To summarize, the above features set forth in claim 1 have the following advantages:

      a.   better functionality of the tokens since even with the gripping wings they can be stacked;

b.   economy of manufacture

c.   improved tactile sensing of the multi-token provided by the gripping wings;

d.   increased visibility of playing status by the indications on the outer surface of the gripping wings.

Features a., b. and d. also interact with parts of the game that is displayed on the gameboard.

Turning now to the rejection, the Examiner relies on applicant's prior patent for teaching of the game and its layout. Applicant does not dispute this. Applicant contends that the invention is in the combination of the game and the novel multi-token.

In comparing the subject matter of the present invention with applicant's prior patent, it is clear that the multi-token provides all of the advantages discussed above. The Examiner recognizes that applicant's prior patent does not teach the novel multi-token and relies on Moore for this feature.

There are substantial differences between the playing pieces shown in the Moore patent as compared to the multi-tokens of the subject invention as set forth in claim 1. For example, claim 1 sets forth that the complete multi-token is an elongated parallelepiped, while Moore's game pieces are cubic shaped. A cube is not an elongated parallelepiped body. A cube has equal sides and not the elongated sides of the elongated parallelepiped. It is true that because of the cubic shape Moore's playing pieces can be stacked. However, it is easier to stack applicant's tokens because the sides are longer.

Also, when considering the use of Moore's playing pieces as compared to the

multi-tokens of the subject invention, there are considerable differences. That is, Moore's playing pieces are used in a capture-type of game, like checkers (see column 2, lines 37-67). There does not appear to be any interaction between any of the indicia on Moore's playing pieces and the parts of the gameboard. In the subject invention the mode of transportation indicia on the sides of the playing pieces correspond to parts of the gameboard. For example, an airplane indicia on a multi-token matches up with a corresponding area of the gameboard having this indicia. In the Moore patent, even referring to Fig. 21 where a boat, airplane and auto are shown on the gameboard, there appears to be no such playing piece/gameboard interaction. Reference is made to the description of Moore's Fig. 21 at column 5, lines 20-55.

The Examiner states at the top of page 3 of the Action that the applicant does not disclose why it is critical for the multi-tokens to be of an elongated parallelepiped shape and, because of this, he concludes that this shape would be a matter of obvious design choice. Applicant urges that "criticality" is not the issue present here. What is present is the question of what advantages the elongated parallelepiped body produces. It is settled law that the Examiner must consider arguments and additional evidence submitted relative to advantages of structure that is disclosed in the application. Reference is made to MPEP 716.02(f).

The advantages of the elongated parallelepiped body as compared to a cube is that it is much easier to stack the former and that the stack will be more stable since there is more surface area in contact. Also, there is more surface area on the flat sides on which

to place indicia.

Also important is the claimed feature of the gripping wings at the ends of the multi-token body. The Examiner recognizes that neither Barry nor Moore discloses such gripping wings. As discussed above, the advantages of the gripping wing structure relates to increasing the tactile utility of the multi-token. This is particularly useful and desirable for people having infirmities such as arthritis, and other neurological impairments.

The Examiner summarily dismisses the important gripping wing feature by concluding "that a person having ordinary skill in the art would have expected the sides of Moor to functionally perform the same, which is to provide sides for moving the game piece". While it is true that Moore's pieces are moved by gripping the sides, the patent does not teach or even remotely suggest the claimed gripping wings that leave a recess between the ends of the elongated parallelepiped body which provide the increased tactile performance as shown by the submitted Exhibits A and B.

Main claim 1 sets forth a novel and advantageous combination that patentably distinguishes over the cited art. There is no logical basis to combine the playing pieces of Moore with the gameboard of the Barry patent since there is no teaching in Moore of interaction between the indicia on such playing pieces and parts of the gameboard as used in the present invention. Even if the combination is improperly made, the structure of claim 1 is not met for the various reasons given above. The novel design of the multi-tokens of the invention, including the gripping wings, provide a number of advantages. Accordingly, claim 1 is clearly patentable and should b allowed.

The other claims depend, in one way or another, from claim 1. In view of the allowability of claim 1, these claims are also patentable and should be allowed.

The other active claims depend, in one way or another, from claim 1 and also should be allowed.
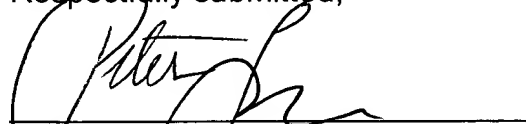
The amendment should be entered since it clearly places the application in condition for allowance.

In view of the above amendments and remarks, it is respectfully requested that the application be reconsidered and that all pending claims be allowed and the case passed to issue.

If there are any other issues remaining which the Examiner believes could be resolved through either a Supplemental Response or an Examiner's Amendment, the Examiner is respectfully requested to contact the undersigned at the telephone number indicated below.

Prompt and favorable action is requested.

Respectfully submitted,

S. Peter Ludwig
Reg. No. 25,351
Attorney for Applicants

DARBY & DARBY, P.C.
Post Office Box 5257
New York, NY 10150-5257
Phone (212) 527-7700

Understanding of Fingernail-Bone Interaction and Fingertip Hemodynamics for Fingernail Sensor Design

Stephen A. Mascaro and H. Harry Asada

d'Arbeloff Laboratory for Information Systems and Technology,
Massachusetts Institute of Technology
smascaro@mit.edu, asada@mit.edu

Abstract

When the human fingertip is pressed against a surface or bent, the hemodynamic state of the fingertip is altered due to mechanical interactions between the fingernail and bone. Normal force, shear force, and finger extension/flexion all result in different patterns of blood volume beneath the fingernail. This phenomenon has been exploited in order to detect finger forces and finger posture by creating a photoplethysmograph "fingernail sensor," which measures the two-dimensional pattern of blood volume beneath the fingernail. In this paper, the anatomical structure of the fingertip is investigated in order to understand the various ways in which the bone and nail interact to alter the hemodynamic state of the fingertip. A qualitative nail-bone interaction model is created and used to explain the different blood volume patterns that result from each stimulus. The model is verified using experimental data from the fingernail sensor. The impact of this study on potential performance and application of the fingernail sensors is discussed.

1. Introduction

Fingertip forces play an increasing role in the fields of robotics, medicine, and virtual reality [1]. They act as bi-directional feedback between human and environment, either mechanical or virtual. Forces applied by a machine or virtual tool are fed back and presented to the human, while forces applied by the human are measured and fed back to the machine or virtual environment. Both application and measurement of fingerpad forces are required, and understanding the mechanics and dynamics of the human fingerpad is important for both.

Several researchers have investigated the mechanics and dynamics of the human fingerpad [2]-[5]. Resulting analyses lead to a better understanding of human grasping and manipulation, characterizations of the human haptic sense, ergonomic design criteria [2], and performance criteria for haptic feedback devices [6]. However only a few studies have taken into account the role of the fingernail in fingerpad behavior [7]. It is well documented in medical literature that the fingernail plays an important role in human grasping and fine manipulation [8], [9].

In addition to applying forces, the fingernail has recently been discovered to be useful for measurement of forces. When forces are applied to the fingerpad, interaction between the fingernail, bone, and tissue alters the hemodynamic state of the finger, creating various patterns of blood volume in the capillaries beneath the fingernail. In previous works, photoplethysmograph fingernail sensors have been designed which optically measure the two-dimension pattern of blood volume beneath the fingernail [10]. These patterns can then be used to predict the fingerpad forces. Normal forces, shear forces, and changes in finger posture have all been shown to result in different blood volume patterns.

In order to better design such fingernail force sensors, it is important to understand the sensing mechanism, including the mechanics of the fingernail-bone interaction and its effect on blood volume. In previous research, the mechanism behind the hemodynamic response to normal force has been quantitatively modeled, but the response to shear force and finger bending were not understood [11].

In this paper, a unified qualitative model will be created that will explain the mechanism behind the blood volume patterns for normal force, shear forces, and finger posture. First, the observable fingernail color patterns that are representative of blood volume are described. Next, relevant structural and vascular anatomy of the fingertip is analyzed and used to create the qualitative nail-bone interaction model. Experimental data from the fingernail sensor is then used to verify the blood volume patterns predicted by the model. Finally, the impact of this study on potential performance and application of the fingernail sensors is discussed.

2. Fingernail Color Patterns

As the human fingertip is pressed down on a surface with increasing force, the blood flow through the fingertip is affected, and a sequence of color changes is observed through the fingernail. In fact, the color change is characteristically non-uniform across the nail, resulting in distinct patterns of color change for different types of forces.

2.1. Normal Touch Force

Figure 1 shows the typical sequence of noticeable color changes with increasing normal force. As the touch force is first increased, the veins in the fingertip are collapsed, causing blood to pool up in the capillaries beneath the nail, resulting in the reddening effect. As the force continues to increase, the force propagates around the bone, collapsing the capillaries at the tip of the nail bed, resulting in a white zone at the tip of the nail.

Figure 2 shows an example of the effect of normal touch force on the fingernail. The pictures on the left show the fingernail coloration under ordinary conditions with no force. The pictures on the right show the coloration with normal force. Just as in Figure 1, the area around the bone is whitened, while the area above the bone is reddened. Digital filtering techniques are used to improve the contrast between red and white zones. In the figures on top, the contrast has been multiplied by five, and in the figures on the bottom, an intensity threshold has been applied.
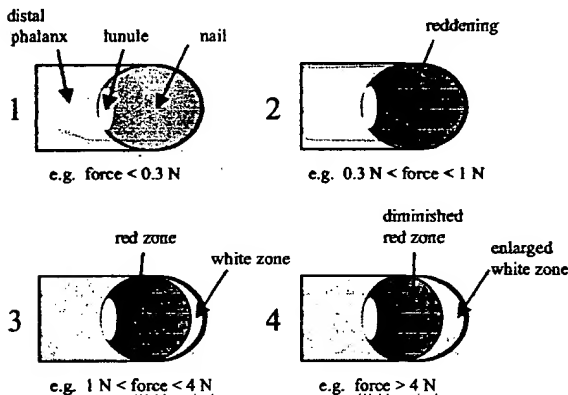
2.2. Change in Posture

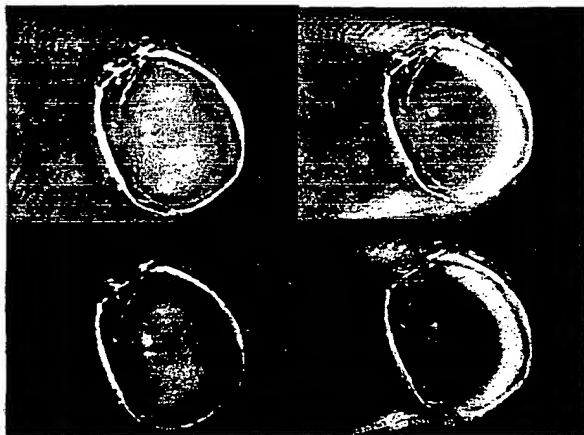Normal touch force is not the only action that results in a change in fingernail color. When the posture of the finger is altered, i.e. the joints of the finger are bent or extended, the color of the finger changes as shown in Figure 3. When the finger is extended, a tension is set up in the tissues of the nail bed that collapses the capillaries. When the finger is bent, that tension is relieved and the capillaries fill with blood again. The color changes shown in Figure 3 are concentrated near the center of the nail, whereas the color changes due to normal touching occur particularly towards the tip of the nail. Therefore it should be possible to distinguish between a touching action and a change in finger posture based on observable changes in fingernail color patterns.

Figure 4 demonstrates the visible effect of finger extension on the fingernail. When the finger is extended, whitening occurs between the bone and the fingernail, especially at the distal end of the bone. When the finger is flexed, the whitening disappears and the entire nail reddens.
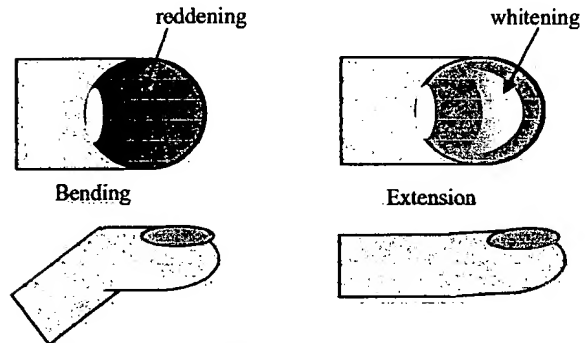

Figure 1. Fingernail colors due to touching.

Figure 3. Fingernail colors due to bending.

Figure 4. Visible effect of extension.

2.3. Shear Force

When shear forces are applied to the palmar surface of the fingertip, yet another set of color patterns result, as shown in Figure 5. If the shear force is applied longitudinally, a tension in the tissues of the nail bed is set up, resulting in either a broad whitening effect over the center of the nail or a white band at the tip of the nail,

Figure 2. Visible effect of normal touch.

depending on the direction. If the shear force is applied laterally, tension in the nail bed creates whitening zones that are asymmetrical.
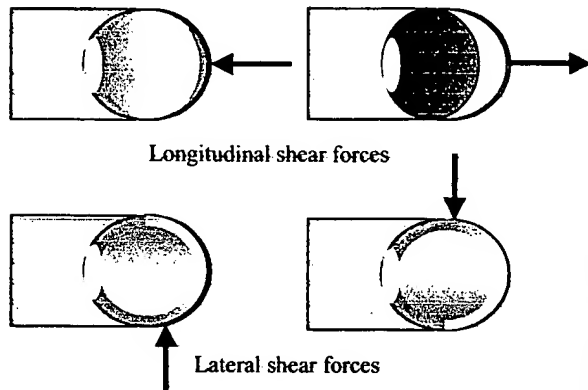

Figure 5. Fingernail colors due to shear.

Figure 6 depicts the visible effect of lateral shear force on the fingernail. In the picture on the left, the shear force is applied from top to bottom, while on the right, the shear force is applied from bottom to top. In both cases, the fingernail whitens around the bone on the far side of the nail toward which the shear vector is pointing, as well as over the bone toward the near side of the shear vector.
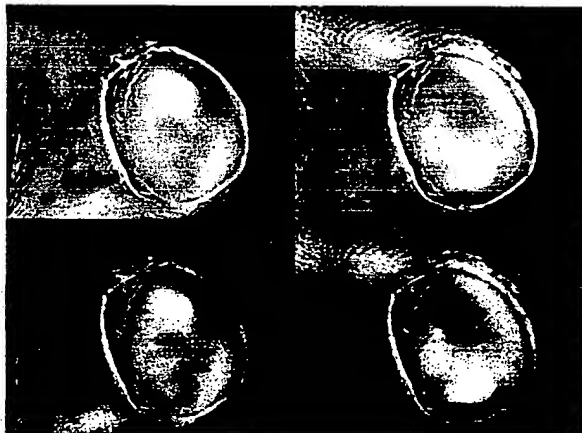

Figure 6. Visible effect of lateral shear force.

Finally, Figure 7 shows the visible effects of longitudinal shear force. The picture on the left depicts shear applied to the finger from left to right (positive by our convention). In this case we see whitening over the bone, but reddening at the tip. The picture on the right depicts shear applied to the finger from right to left (negative by our convention). In this case, we see whitening around the bone, which is not significantly different from the patterns caused by normal force alone.

Since the patterns for lateral shear force are distinctly asymmetrical, it should be easy to distinguish from normal

touching and bending. However, longitudinal shear forces may present a greater challenge to distinguish. When the longitudinal shear is applied inward (top right of figure), the whitening zone is similar to that of bending, but extends all the way to the lateral edges of the nail. When the longitudinal shear force is applied outward (top left of figure), the whitening zone is almost indistinguishable from that of normal touching, making this perhaps the most challenging force to measure. However, there may be subtle variations in blood volume that are more visible to optoelectronic sensors than to the naked eye.
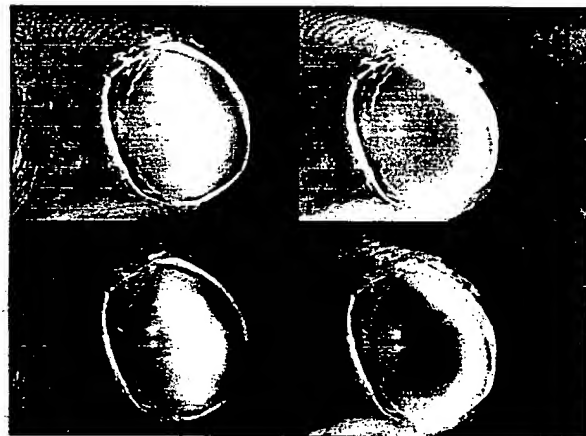

Figure 7. Visible effect of longitudinal shear.

3. Anatomy of Fingertip and Nail Bed

In order to explain the mechanism behind the changes in color of the fingernail, it is necessary to thoroughly understand the relevant anatomy and physiology of the fingertip. First, the anatomical structure and function of the fingertip and fingernail is investigated. Secondly, the blood flow in the fingertip and fingernail bed will be investigated.

3.1. Structure of the Fingertip and Fingernail

Details of the anatomical structure of the fingertip can be found in several references such as [8], [9], [12]. The top portion of Figure 8 shows a saggital cross-section of the fingertip. The bone of the distal phalanx is surrounded beneath by the soft deformable tissue of the pulp and above by the nail unit. The nail plate is attached to the bone by the anterior ligament (AL), the posterior ligament (PL), and the bed mesenchyme (BM), the latter having an almost ligamentary or tendon-like character [8]. This anchoring serves to maintain the positional relationships and distances between the matrix, bed, hyponychium, and bone, which are critical for nail health and functionality. The nail plate is generated by the matrix, grows up and emerges out from under the proximal nail fold at the

eponychium, curves over the nail bed, and separates from the fingertip at the hyponychium. It is transparent and colorless, acting as a window into the nail bed.
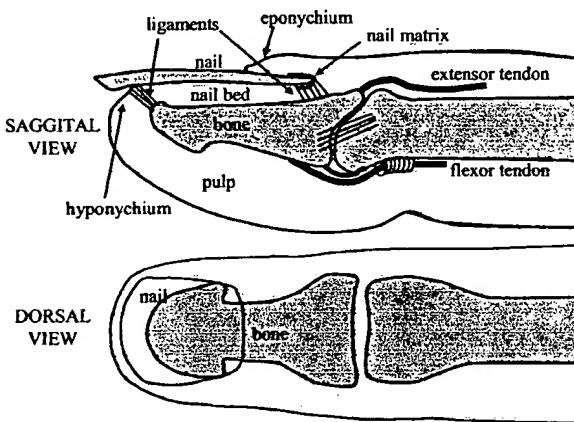

Figure 8. Structural anatomy of the fingertip.

Figure 8 also shows the actuation mechanism of the fingertip. Movement of the finger and forces at the fingertip are effected by means of a network of flexor and extensor tendons, [9]. The extensor tendons pull the finger up into an extended position, while the flexor tendons pull the finger down into a bent or flexed position.

3.2. Blood Supply of the Fingertip and Nail Bed

According to [8], after application of pressure to the pulp, this middle nail bed turns pinker while the distal bed becomes whiter, which supports the role of the bed vasculature as the main source of the pink color of the bed.

A variety of details on the vascular anatomy of the fingertip can be found in several sources such as [8],[9],[13]-[16]. The nail bed is richly vascularized with blood flowing from the digital arteries into a network of arterioles, through capillary loops just under the surface, and back out through the venules to the digital veins. Figure 9 shows a diagram of the principal arteries and veins. The main digital arteries divide into a network of smaller arteries that run principally above the bone, which is connected to the fingernail via a strong matrix of collagen and elastic fibers, as described in the previous section. As a result, the arteries underneath the nail are protected from touch pressure, allowing uninterrupted supply of blood to the capillaries under the nail. However, the flow of blood out of the fingertip relies largely on the lateral ramifications of the digital veins shown in the figure [16]. In addition, the veins are generally larger and more compliant than the arteries, leaving them susceptible to collapse by touch pressure. As a result, when touch pressure is applied to the fingertip, the veins are collapsed, causing blood to pool up in the capillaries underneath the nail.
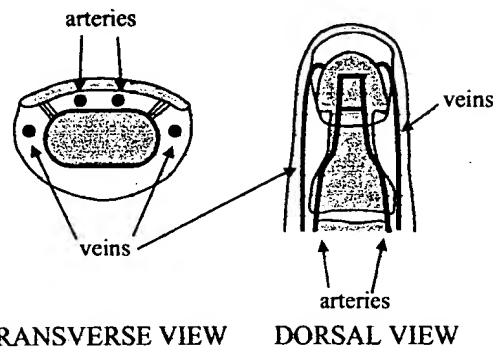

TRANSVERSE VIEW   DORSAL VIEW

Figure 9: Vascular anatomy of the fingertip.

The capillaries run longitudinally under the nail bed and are twice as long and twice as numerous as those in the pulp on the palmar side of the fingertip [13]. Under normal conditions, the blood in the capillaries is rich in oxygen and therefore red. Thus the blood that pools up in the capillaries of the nail bed is highly visible and is responsible for the reddening effect described earlier. However the capillaries under the nail at the tip of the finger are not protected by the bone. Thus touch pressure can propagate around the tip of the bone, causing these capillaries to collapse and pushing all of the blood out of them. This results in the whitening effect described earlier.

A final relevant detail is that the arteries are tortuous and coiled while the veins are not [15]. Thus when the finger is bent, the veins become kinked, while the arteries merely uncoil.

4. Fingernail-Bone Interaction Model

4.1. Basic Mechanism

As described in the previous section, and shown in Figure 8, the fingernail is connected to the bone of the distal phalanx by a matrix of strong fibers, especially around the perimeter of the nail, which prevent the nail from detaching from the bone, even under very high tension. However these fibers do not prevent the nail from being compressed against the bone. Touch forces and posture are maintained through tension in the flexor and extensor tendons, which are attached at the proximal end of the bone. The tendons are thus able to exert torque on the bone but do not directly affect tension in the tissue of the fingertip.

The bone itself has a distinctive arrowhead shape with protuberances at both ends where the fibers are attached. The bone does not extend all the way to the hyponychium

where the nail detaches from the skin. This geometry is important in determining the regions of the nail bed that are affected by various forces within the fingertip. The shape and position of the bone and its effect on the nail bed capillaries is evidenced by Figure 10. On the left, the finger is pressed down against a flat surface. The profile of the bone is visible as the region of red where the capillaries are protected from collapsing due to the pressure. On the right, the nail is pressed against a transparent surface. In this case the profile of the bone is visible as the region of white where the capillaries between the nail and bone are compressed and collapsed, which also confirms the inability of the nail fibers to support compression.
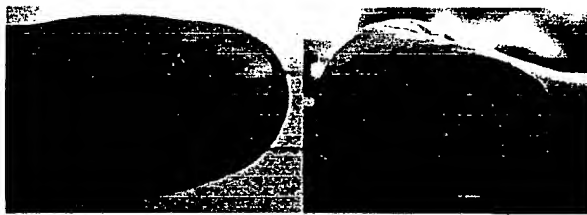

Figure 10. Nail-bone interaction.

The important characteristics of the basic bone-nail interaction model can be summarized as the following:

- The bone (distal phalanx) has a distinctive arrowhead shape with protuberances at both ends.
- The fiber matrices between nail and bone support tension but not compression.
- Tension in the tissue allows blood volume to increase while compression causes blood volume to decrease

This basic model is now ready to be applied to explain the mechanism behind each of the various types of touch force and posture.

4.2. Normal Force

Figure 11 depicts the nail-bone interaction and its hemodynamic effect for normal force. The top diagrams depict the ordinary state of the fingertip when no force is applied. The tissue is shaded lightly to indicate it is neither in tension nor compression. The transverse and dorsal views also depict the primary arteries (over the bone) and veins (beside the bone). The bottom diagrams show a z-force exerted beneath the fingertip and its corresponding reaction force exerted by the bone, which is achieved by tension in the flexor tendon. These forces compress the tissue of the pulp between the bone and the surface, as depicted by the area in white. Note that the compression extends to the area around the bone as well as beneath it. This is because the nail bed fibers are in tension and pull the nail down with the bone, compressing all the tissue that is around the bone but beneath the nail.

This includes the lateral aspects of the finger where the primary veins lie. Thus the veins are collapsed, causing blood to pool up in the protected capillaries between the nail and the bone, as depicted by the area shaded darkly.
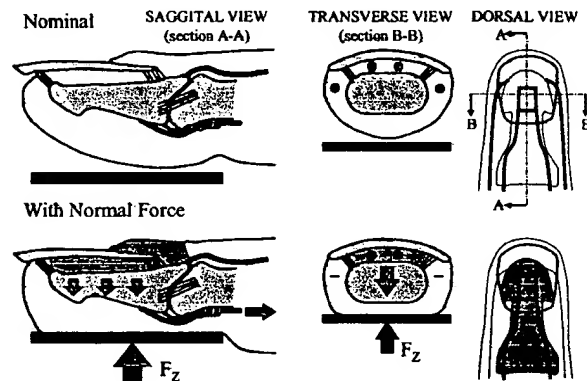

Figure 11. Normal touch mechanism.
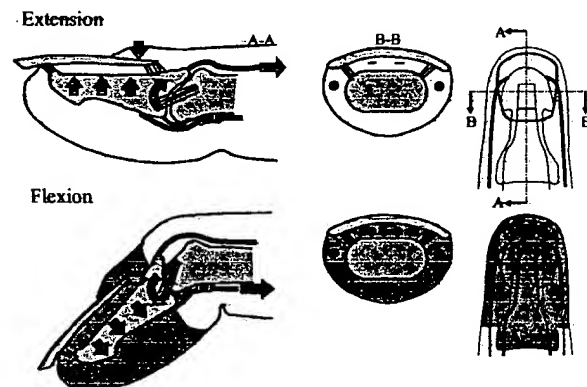
4.3. Extension/Flexion

Figure 12. Bending mechanism.

Figure 12 depicts the nail-bone interaction and its hemodynamic effect for finger extension and flexion. During extension, the extensor tendon pulls the bone upward against the fingernail, which is held in place by a reaction force from the proximal nail fold. Since the fibers of the nail bed do not support compression, the capillaries are collapsed between the bone and the nail, especially above the bony protuberance at the distal end of the bone.

When the finger is flexed, the flexor tendon pulls the bone down away from the nail, relieving the compression between the nail and bone. Since the nail bed fibers are now in tension, the fingernail maintains a normal position relative to the bone. However, additional reddening occurs throughout the fingertip since flexion of the finger kinks the veins, causing blood to pool up in the capillaries throughout the fingertip.

4.4. Lateral Shear Force

In the case of lateral shear force, the bone-nail interaction is more complex, as depicted in Figure 13. In order to apply shear, a normal force must be simultaneously exerted in order to allow for friction. It has already been established that when normal force is applied, the area around the bone is compressed and whitened. When lateral force is exerted in addition to normal force, a lateral reaction force is maintained in the bone by the ligaments of the joint, and the tissue of the pulp between the bone and surface experiences a shear force that pulls the tissue toward the far side of the shear vector. Thus the tissue at the far side becomes bunched up around the nail due to shear and whitened due to compression by the normal force. However, on the near side of the shear vector, the tissue is pulled away from the nail by the shear force. The tension of this pulling action prevents compression of the tissue at the near side, resulting in reddening. Furthermore, the tension at the near side pulls the nail down on top of the bone there resulting in whitening.
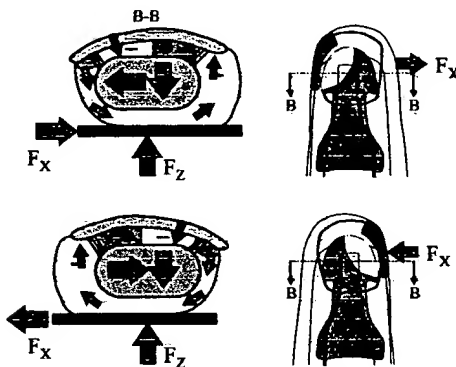

Figure 13. Lateral shear mechanism.

4.5. Longitudinal Shear Force

Unlike lateral shear force, the mechanism of longitudinal shear force is different for positive and negative forces, as depicted in Figure 14. When force is applied in the positive direction, as depicted in the bottom diagrams, the mechanism is similar to lateral shear. Applied shear and reaction force in the bone pulls the tissue proximally. At the distal end of the nail, the tissue is pulled away, generating tension and preventing the capillaries from collapsing, resulting in reddening. However the tension pulls the nail down on top of the bone, generating a whitening zone between the nail and bone. When force is applied in the negative direction, as depicted in the top diagrams, the tissue is bunched up at the distal end of the nail due to the shear and compressed due to normal force.
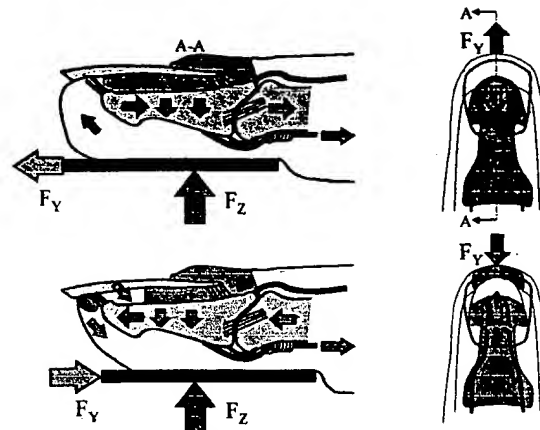

Figure 14. Longitudinal shear mechanism.

5. Verification and Applications

5.1. Experimental Verification

In order to verify that the blood volume patterns predicted by the nail-bone interaction model are accurate, experimental data is collected using the fingernail sensor developed in previous work [10]. Figure 15 shows the arrangement of the optical components of the fingernail sensor. There are eight photodiodes in a two-dimensional array with six LEDs in between. The signal from each photodiode is dominated by the local blood volume beneath the fingernail.
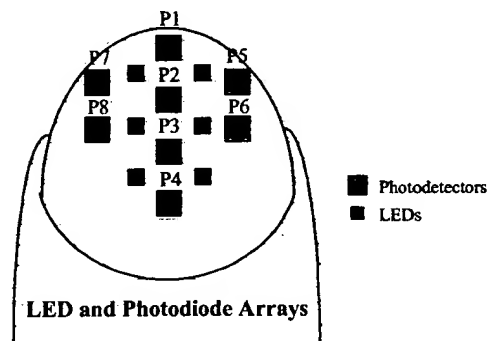

Figure 15. Sensor arrangement.

Figure 16 to Figure 19 show the responses of the eight photodiodes to normal force, bending, lateral shear force, and longitudinal shear force. In each figure, the eight plots are arranged in the same formation as the photodiodes on the fingernail. In each case, the human subject was asked to slowly vary the stimuli of interest over several cycles while holding the others constant. The photodiode signals are plotted vs. the applied stimuli. The forces are measured using a three-axis force sensor and the joint angle is measured using a video camera. The hysteresis in

each of the curves is due in part to the fact that the other three stimuli are not held perfectly constant while the stimuli of interest is being varied.
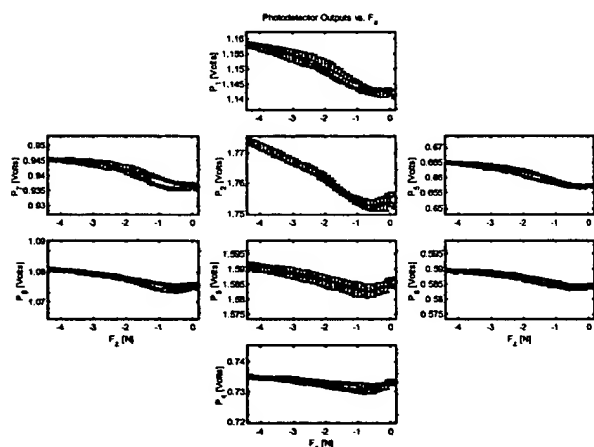

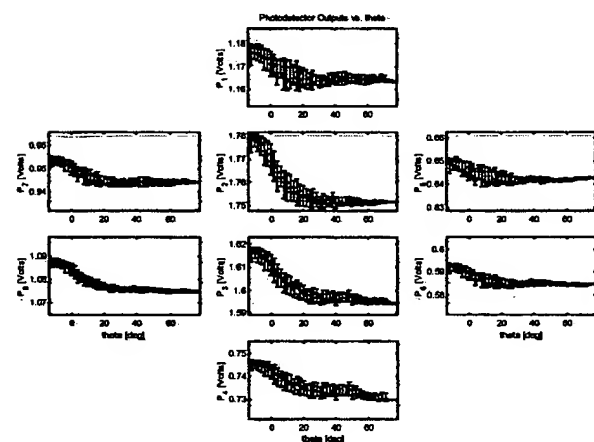Figure 16. Sensor response to normal force.

Figure 17. Sensor response to extension/flexion.

When the magnitude of normal force increases, the photodiode signals increase, particularly towards the front and sides of the fingernail. This is because the whitening causes more light to be reflected, increasing the photodiode response. The front-most photodiode levels off first because it is the first to go completely white. As more force is applied, the white zone grows proximally and the middle photodiodes continue to increase.

When the finger is flexed (increasing joint angle), the middle of the nail is reddened and the photodiode signals decrease, particularly in the middle of the nail. For extension, the nail whitens and the signals increase.

When lateral shear is applied, the photodiodes now act in a laterally asymmetric pattern as expected. For positive

lateral shear (i.e. shear applied from right to left), the distal right side reddens (decreasing signal) and the distal left side whitens (increasing signal), just as predicted by the model. Likewise, for negative lateral shear (left to right), the distal left side reddens and the distal right side whitens. The photodiode at the front middle stays whitened, while the photodiodes in the rear fluctuate as the proximal whitening zone shifts around over the bone.
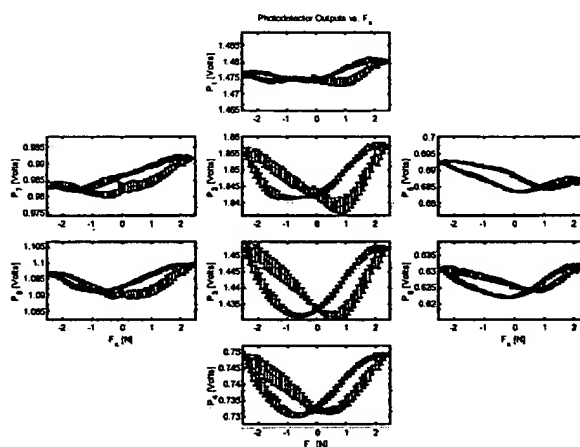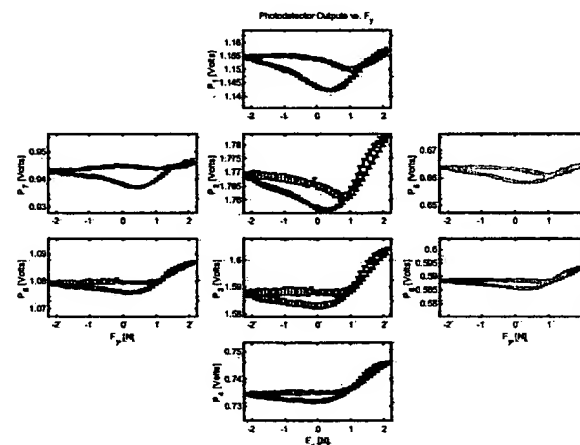

Figure 18. Sensor response to lateral shear.

Figure 19. Sensor response to long. shear.

When longitudinal shear is applied in the positive direction (front to back), the photodiodes signals all increase due to the broad whitening zone in the middle of the nail. However, when longitudinal shear is applied in the negative direction (back to front), the photodiode signals tend to remain the same or increase only slightly. Thus negative longitudinal shear will be difficult to distinguish based on sensor readings.

5.2. Impact on Applications of Fingernail Sensor

Since the fingernail sensor is capable of measuring shear force in addition to normal force, a potential application is to use the fingernail sensor as a wearable computer mouse, as shown in Figure 20. This is especially feasible since the sensors are most sensitive in the range of 0 to 2 N, which is comfortable for a human to apply on a continuous basis.

However, because both the model and experimental evidence suggest that negative longitudinal shear may be difficult to detect, the wearable mouse application should be designed to function based only on normal force, lateral shear, and positive longitudinal shear. It is possible that the two axes of cursor motion could be controlled by lateral shear and some combination of normal force and longitudinal shear. If the human presses the finger against the side of the computer monitor, then predicted normal force could be intuitively used to control horizontal cursor position, while predicted lateral shear force could be used to control vertical cursor position. Clicking would be achieved by dynamic tapping or by using a second finger.
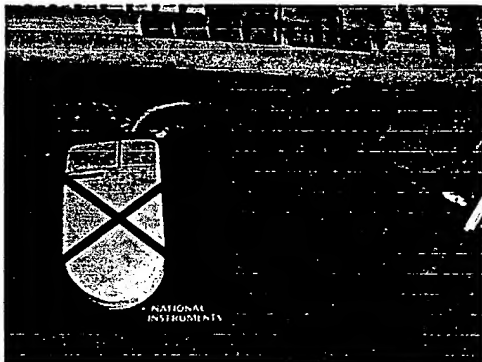

Figure 20. Wearable mouse application.

6. Conclusions

In conclusion, this paper developed a unified qualitative model that explains the fingernail-bone interaction and resulting blood volume patterns that occur in the fingernail bed when various forces and changes in posture are applied to the fingertip. This model is useful in understanding the measurements obtained using the fingernail sensor and designing sensor applications. Using the model, the sensor could be redesigned with an optimal configuration of photodiodes for distinguishing the various patterns of blood volume resulting from normal force, finger bending, lateral shear force, and longitudinal shear force. The understanding of the nail-bone interaction should also prove to be useful for understanding human grasping and manipulation. In

future work, a quantitative model of the nail-bone interaction will be developed.

References

[1] J. Webster, Ed., *Tactile Sensors for Robotics and Medicine.* New York: Wiley, 1988.

[2] D.T.V. Pawluk and R.D. Howe, "Dynamic Lumped Element Response of the Human Fingerpad," *J. Biomechanical Engineering*, vol. 121, pp. 178-183, 1999.

[3] D.T.V. Pawluk and R.D. Howe, "Dynamic Contact of the Human Fingerpad Against a Flat Surface," *J. Biomechanical Engineering*, vol. 121, pp. 605-611, 1999.

[4] E.R. Serina, C.D. Mote, Jr., and D. Rempel, "Force Response of the Fingertip Pulp to Repeated Compression-Effects of Loading Rate, Loading Angle and Anthropometry," *J. Biomechanics*, vol. 30, no. 10, pp. 1035-1040, 1997.

[5] R.J. Gulati and M.A. Srinivasan, "Human Fingerpad Under Indentation I: Static and Dynamic Force Response," *ASME Bioengineering Conf.*, BED-Vol. 29, pp. 261-262, 1995.

[6] U. Singh and R.S. Fearing, "Tactile After-Images from Static Contact," *Proc. ASME Dynamic Systems and Control Division*, vol. 64, pp. 163-170, 1998.

[7] H.-Y. Han, A. Shimada, and S. Kawamura, "Analysis of Friction on Human Fingers and Design of Artificial Fingers," *Proc. IEEE Int. Conf. Robotics and Automation*, pp. 3061-3066, 1996.

[8] R.K. Scher and C.R. Daniel, III, *Nails: Therapy-Diagnosis-Surgery.* Philadelphia, W.B. Saunders, 2nd edition, 1990.

[9] R. Tubiana, Ed., *The Hand*, vol. 1, Philadelphia, W.B. Saunders, 1981.

[10] S. Mascaro and H.H. Asada, "Finger Posture and Shear Force Measurement using Fingernail Sensors: Initial Experimentation," *Proc. IEEE Int. Conf. Robotics and Automation*, pp. 1857-1862, 2001.

[11] S. Mascaro and H.H. Asada, "Fingernail Touch Sensors: Spatially Distributed Measurement and Hemodynamic Modeling," *Proc. IEEE Int. Conf. Robotics and Automation*, pp. 3422-3427, 2000.

[12] R. Baran, et al., *Diseases of the Nails and their Management*, 2nd ed., R. Baran and R. P. R. Dawber, Eds. Oxford: Blackwell Scientific, 1994.

[13] R. Wolfram-Gabel and H. Sick, "Vascular networks of the periphery of the fingernail," *J. of Hand Surgery*, vol. 20B, no. 4, pp. 488-492, 1995.

[14] E. G. Zook, A. L. Van Beek, R. C. Russell, and M. E. Beatty, "Anatomy and physiology of the perionychium: a review of the literature and anatomic study," *J. of Hand Surgery*, vol. 5, no. 6, pp. 528-536, 1980.

[15] D. O. Smith, O. Chikayoshi, C. Kimura, and K. Toshimori, "Artery anatomy and tortuosity in the distal finger," *J. of Hand Surgery*, vol. 16A, pp. 297-302, 1991.

[16] D. O. Smith, O. Chikayoshi, C. Kimura, and K. Toshimori, "The distal venous anatomy of the finger," *J. of Hand Surgery*, vol. 16A, pp. 303-307, 1991.

Finger Posture and Shear Force Measurement using Fingernail Sensors: Initial Experimentation

Stephen Mascaro and H. Harry Asada

d'Arbeloff Laboratory for Information Systems and Technology
Department of Mechanical Engineering
Massachusetts Institute of Technology
Cambridge, MA 02139, e-mail: smascaro@mit.edu, asada@mit.edu

Abstract

A new method for measuring both the posture of human fingers and shear force at human fingertips is presented. Instead of using a traditional electronic glove with bending sensors embedded along the finger and shear sensors embedded beneath the fingertip, a wearable fingernail sensor is used to measure resulting changes in coloration of the fingernail. Since the sensor is mounted on the fingernail, finger posture can be measured without wearing a glove that hampers the motion of the fingers. Similarly, shear forces can be measured without covering the finger pad and obstructing the human's natural haptic sense. In the past, fingernail sensors with a one-dimensional array of photodetectors have been used to measure normal touching forces at the fingertip. A new fingernail sensor with a two-dimensional spatial array of photodetectors is constructed in order to measure finger posture and shear forces. Experiments are performed in order to measure the outputs of the photodetectors in response to changes in finger posture and applied normal and shear forces. Analysis is then performed to correlate the outputs to the inputs and provide a means of estimating normal forces, shear forces, and changes in finger posture.

1. Introduction

There is an increasing need for measuring both finger posture and forces acting between human hands and the environment. Finger posture is usually measured by wearing electronic gloves, which have been increasingly used in the robotics and virtual reality communities for a variety of human-machine interactions [1]. External finger forces are traditionally measured by placing force-sensing pads at the fingertips. A wide variety of such pads have been developed in the past for applications in robotics and medicine [2], using resistive, capacitive, piezoelectric, or optical elements to detect force [3], [4], [5]. These pads have often been placed in electronic gloves in order to monitor human skills and behavior during manipulation, perform teleoperation, and interact with machines and virtual environments [6], [7], [8], [9], [10], [11].

Shear forces, or sliding forces in the plane of the contacting surface, play an important role in human manipulation of objects. Shear forces, however, are very difficult to measure without interfering with the human's haptic sense. For robotic hands, several clever designs of shear force sensors have been presented. Howe and Cutkosky developed a superior shear force tactile sensor for detecting slip and surface texture [12]. Novak proposed a shear force sensor design using a capacitive sensor array [13]. Unfortunately these shear force sensors must be placed between the fingertip and the environment, and are therefore inappropriate for measuring human finger forces. A critical problem with traditional electronic gloves and force sensors in general is that they cover the fingers, blocking the natural human haptic sense as well as restricting the natural bending motion of the fingers.

In a previous paper by the authors [14], a new approach to the detection of finger forces was presented to completely eliminate any impediment to the natural haptic sense. Namely, the finger force is not measured by placing a sensor pad between the finger skin and the environment surface, but is instead detected by an optical sensor mounted on the fingernail. This allows the human to touch the environment with bare fingers and perform fine, delicate tasks using the full range of haptic sense. Miniaturized optical components and circuitry allow the sensor to be disguised as a decorative fingernail covering. A lumped-parameter hemodynamic model was created in order to explain the color change at two locations under the fingernail.

In this paper, a new fingernail sensor is constructed in order to allow for measurement of finger posture and shear forces in addition to normal touching forces. This new fingernail sensor has a two-dimensional spatial array of photodetectors for measuring shear forces along two different axes. Firstly, this paper describes the various color changes that result from touching, bending, and shear forces. An experimental platform is then assembled in order to measure the response of the fingernail sensor to known finger postures and shear forces. Experimentation and analysis are performed in order to relate the outputs of the fingernail sensor to the finger posture and shear force inputs. Based on the analysis, a method for simultaneously estimating normal forces, shear forces, and changes in finger posture is presented. Applications to a human-machine interface and a computer pointer are discussed.

2. Principle

2.1 Color Change Due to Touching

As the human fingertip is pressed down on a surface with increasing force, the blood flow through the fingertip is affected, and a sequence of color changes is observed through the fingernail. In fact, the color change is characteristically non-uniform across the nail, resulting in distinct patterns of color change. These color patterns can be measured by placing arrays of light emitting diodes and photodetectors on the nail as shown in Figure 1. The output of the photodetectors is proportional to the intensity of reflected light, which depends on the volume of blood in the nail bed.
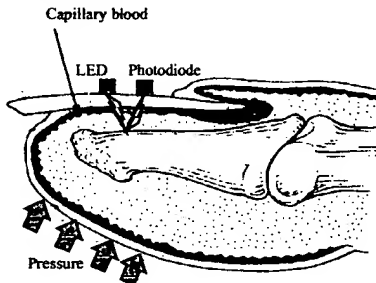
Figure 1: Sensing Principle (picture adapted from [15])

Figure 2 shows the typical sequence of noticeable color changes with increasing force. As the touch force is first increased, the veins in the fingertip are collapsed, causing blood to pool up in the capillaries beneath the nail, resulting in the reddening effect. As the force continues to increase, the force propagates around the bone, collapsing the capillaries at the tip of the nail bed, resulting in a white zone at the tip of the nail.
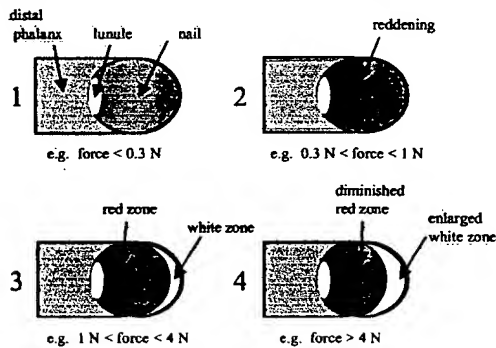

Figure 2: Fingernail Color Change Due to Touching

A variety of descriptions of the anatomy and physiology of the fingertip can be found in medical literature [16], [17], [18], [19], [20]. In previous work [15], the mechanism of these color changes was discussed in more detail and an anatomically based dynamic model was created in order to explain the underlying changes in blood volume. However, normal touch force is not the only action that results in a change in fingernail color. Alterations in finger posture as well as application of shear force result in different color patterns than those shown above.

2.2 Color Change Due to Bending/Extension

When the posture of the finger is altered, i.e. the joints of the finger are bent or extended, the color of the finger changes as shown in Figure 3. When the finger is extended, a tension is set up in the tissues of the nail bed that collapses the capillaries. When the finger is bent, that tension is relieved and the capillaries fill with blood again. Creasing of the veins during bending may also contribute to blood pooling up in the capillaries.
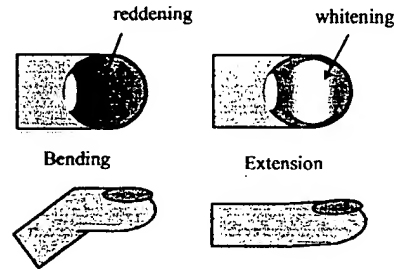

Figure 3: Fingernail Color Change Due to Bending

The color changes shown above are concentrated near the center of the nail, whereas the color changes due to normal touching occur particularly towards the tip of the nail. Therefore it should be possible to distinguish between a touching action and a change in finger posture based on observable changes in fingernail color patterns.

2.3 Color Change Due to Shear

When shear forces are applied to the palmar surface of the fingertip, yet another pattern of color changes result, as shown in Figure 4. If the shear force is applied longitudinally, a tension in the tissues of the nail bed is set up, resulting in a broad whitening effect over the front of the nail. If the direction of the shear force deviates in either direction from the longitudinal axis, then the white zone shifts towards the right or left of the nail as shown.
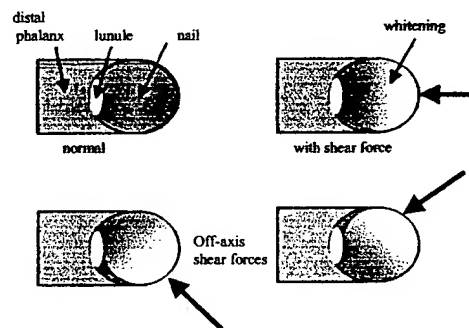

Figure 4: Fingernail Color Change Due to Shear

Unlike the color change due to bending/extension, the white zone due to shear is concentrated toward the front of the nail. However the white zone for shear extends much farther back than in the case of normal touching force. Therefore it should be possible to distinguish shear forces from bending/extension as well as from normal touching.

3. Experimental Apparatus and Method

3.1 Fingernail Sensor Apparatus

In order to recognize normal touch force, bending/extension, and shear forces (both longitudinal and lateral), it is necessary to measure the color of the fingernail using a 2-dimensional spatial array of photodetectors. Figure 5 shows a picture of the fingernail sensor that is used for experimentation. The first picture shows the bottom side of the sensor, where the 2-D array of photodiodes is mounted towards the end of the sensor. Four photodiodes run along the longitudinal axis of the nail with two additional photodiodes on either side for a total of eight photodiodes. Six light emitting diodes are distributed evenly between the photodiodes in order to illuminate the entire nail bed with infrared light at the isobestic wavelength (770nm). The second picture shows the top of the nail sensor, where the photodiode signals are amplified and then sent to an analog-to-digital converter.
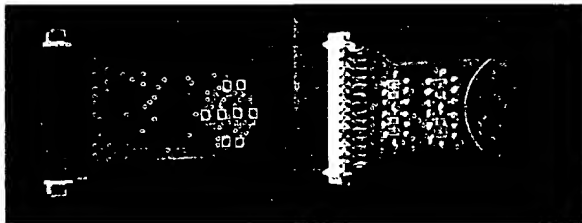

Figure 5: Fingernail Sensor with 2-D Array of Photodetectors

After the optical and electrical components are in place as shown in Figure 5, the bottom side is molded to the shape of the human fingernail using transparent epoxy. The top is covered with opaque epoxy to shield the sensor from ambient lighting. The sensor is then attached to the fingernail (as seen in Figures 6 and 7) using special transparent double-sided adhesive tabs. Thin wires then connect the signals to the wrist and then to the A/D converter and power supply.

3.2 Posture Measurement

In order to experiment with finger posture, it is necessary to be able to measure the angles of the joints of the finger while measurements are simultaneously taken from the fingernail sensor. The easiest method would be to wear an electronic glove; unfortunately such gloves constrict the fingers and interfere with the adhesion of the sensor to the nail. Therefore the fingers are left free and a video tracking system is used instead, as shown in Figure 6. A pair of colored markers is placed on each joint of the finger and video is taken continuously during the experiment. An image processing algorithm is then used off-line to track the centroids of the markers and compute the angle of each joint for each time index. The clock on the computer monitor is used to synchronize the time index of the joint angle measurements to that of the photodetector measurements.
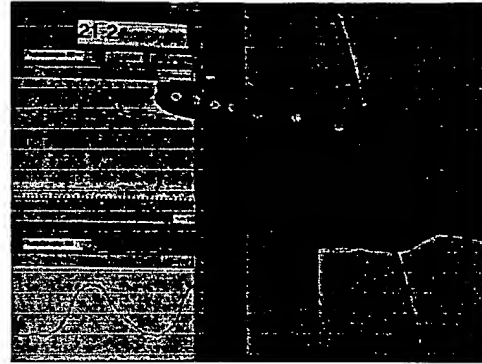

Figure 6: Completed Fingernail Sensor and Video Tracking System for Posture Measurement

3.3 Force Measurement

In order to experiment with shear force, it is necessary to be able to measure the shear forces that are applied to the finger along both the X-axis and Y-axis as well as the normal touching force along the Z-axis. Figure 7 shows a picture of the force measurement system that is used. A Nano17 6-axis force/torque transducer from ATI Automation is used in order to measure forces in the X, Y, and Z directions. The shear forces F_X and F_Y have a sensing range of $\pm$ 12 N and a resolution of 0.8×10^{-3} N. F_Z has a range of $\pm$ 17 N and a resolution of 1.6×10^{-3} N. A rubber pad is placed between the finger and the sensor in order to maximize the coefficient of friction and thus decrease the dependence of the shear force on the normal force.
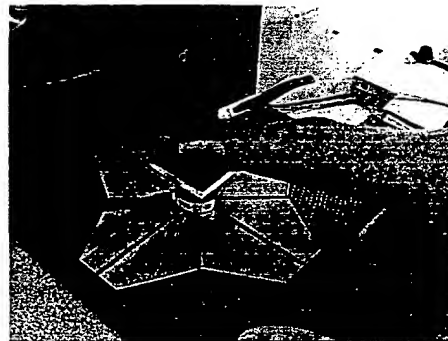

Figure 7: Force Measurement Platform

Ideally, the experiments would be designed so that the finger joints would be held in place while an automated apparatus applies precise shear forces. Unfortunately, a device that would hold the finger in place would put pressure on the finger and affect the blood flow, thus affecting the nail color. Therefore, the human must be relied upon instead to apply the shear forces as precisely as possible. A visual feedback system consisting of gauges on a computer monitor is used to display to the human in real-time the forces that are applied as the finger is pressed on the platform.

4. Experimental Results

4.1 Results for Posture Measurement

Figures 8 through 10 show the results of experiments for finger posture measurement. Starting from a fully bent position, the finger is first fully extended and then fully bent once again. The responses of each of the eight photodetectors are shown in Figure 8. The plots are arranged in the figure to reflect the relative positions of the photodetectors on the fingernail. As shown by the data, the photodetector outputs all respond in phase with the bending.
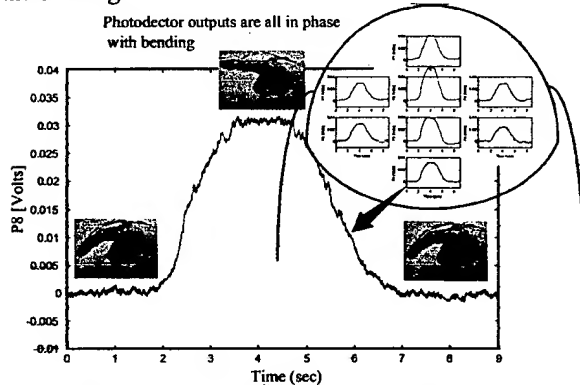
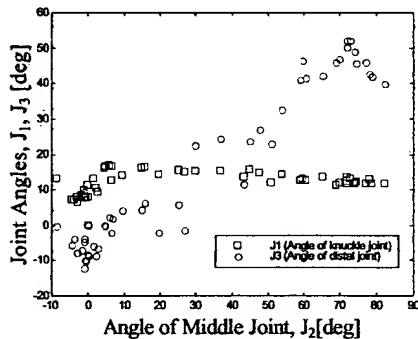

Figure 8: **Response to Finger Bending**

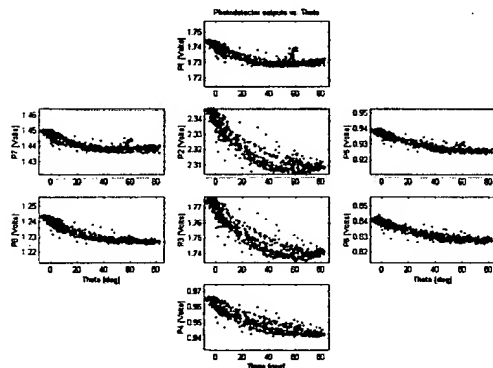**Figure 9:** **Correlation of Joint Angles**

Figure 10: **Sensor Output vs. Bend Angle**

Using the video tracking system shown in Figure 6, the joint angles were computed from video frames spanning the bending range of the finger. The finger consists of three joints, not all of which can be flexed independently.

Figure 9 shows the correlation between the joints using data from the experiment. Since the knuckle joint can be flexed independently of the other two and does not appear to influence the photodetector outputs, the knuckle angle J_1 is held constant for this experiment. The middle and distal joints, J_2 and J_3, cannot be flexed independently and have a roughly linear dependence, as shown in Figure 9. Therefore, the photodetector outputs can be treated simply as a function of J_2, and are plotted as such in Figure 10, showing a characteristic pattern of sensor outputs for bending.
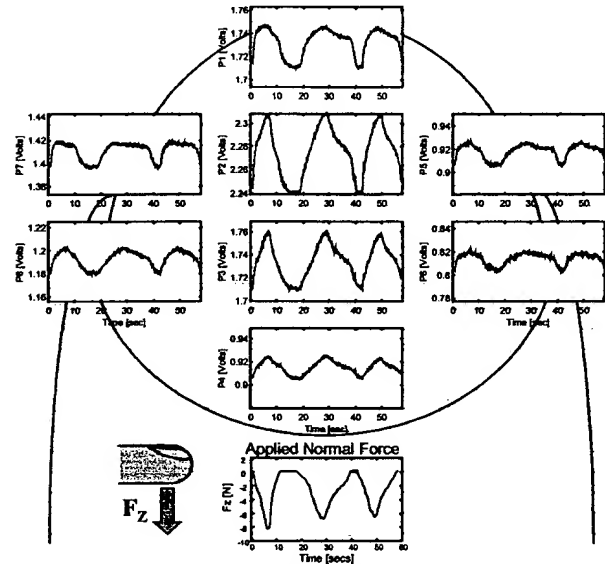
4.2 Results for Force Measurement

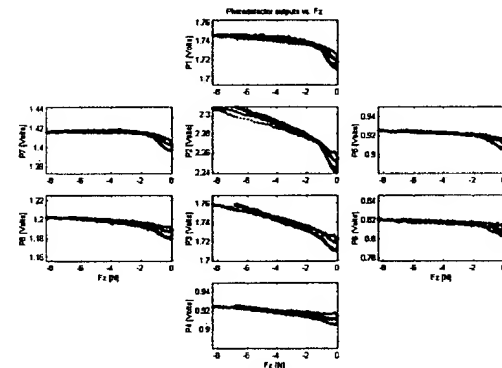**Figure 11:** **Response to Normal Force**

Figure 12: **Sensor Output vs. Normal Force**

Figures 11 and 12 show the results of experiments for measurement of normal force, F_Z. The finger is slowly pressed down on the measurement platform with increasing force and then slowly lifted up again for several cycles. The responses of the photodetectors are plotted vs. time in Figure 11. The normal force F_z is measured by the 6-axis force sensor and is shown at the bottom of Figure 11. In Figure 12, the photodetector outputs are plotted as a function of F_Z, showing a characteristic pattern of sensor outputs for normal force.

This pattern is distinguishable from that of bending by the differences in curvatures and slopes.

Figures 13 and 16 show the results of the experiments for shear force measurement. First, the human applies a periodic lateral shear force (magnitude~3 N, period~0.5 sec) to the palmar surface of the fingertip. The responses of the photodetectors are shown in Figure 13 along with the applied shear force. In this case, unlike the cases of finger bending and normal force, the photodetectors do not all respond in phase. The photodetectors on the left side of the nail react in phase with the shear force while the photodetectors on the right side of the nail react 180 degrees out of phase with the shear force. In Figure 14, the photodetector outputs are plotted as functions of the applied lateral shear force, F_X, showing a characteristic pattern of sensor outputs for lateral shear. The opposite slopes for photodetectors 5 and 7 make this pattern easily distinguishable from the patterns for bending and normal force.
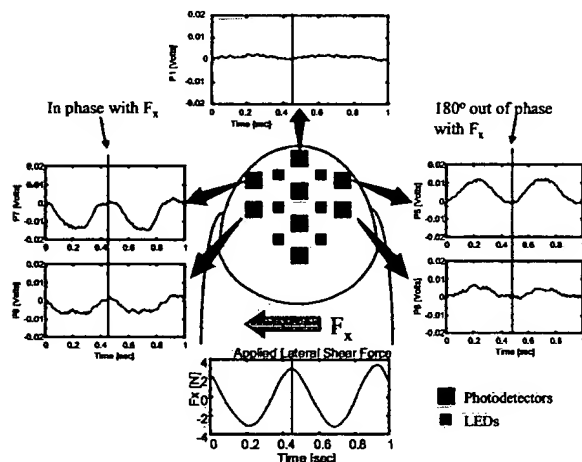

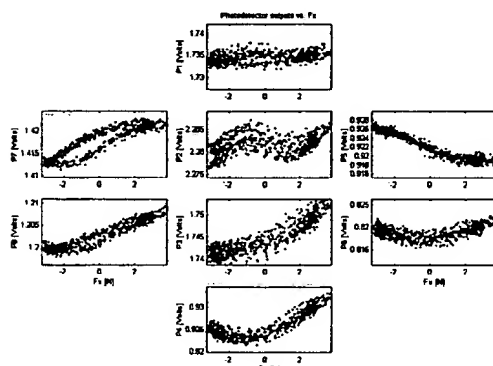Figure 13:   Response to Lateral Shear

Figure 14:   Sensor Output vs. Lateral Shear

Next, the human applies a periodic longitudinal shear force (magnitude~3 N, period~0.5 sec) to the palmar surface of the fingertip. The responses of the photodetectors are shown in Figure 15 along with the applied shear force. In this case the responses all seem to be in phase, but their behavior is much more non-linear. This is more evident in Figure 16, where the

photodetector outputs are plotted as functions of the applied longitudinal force, F_Y, showing a characteristic pattern of sensor outputs for longitudinal shear. The non-linear v-shaped curves make this pattern easily distinguishable from bending, normal force, and lateral shear force.
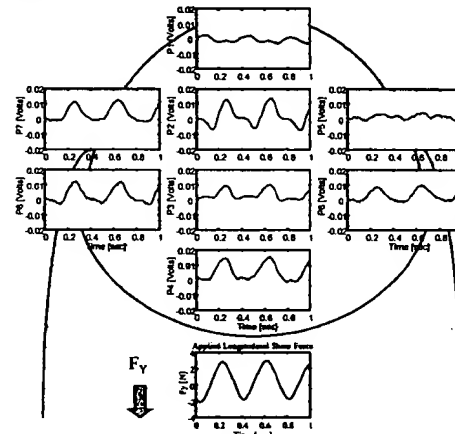

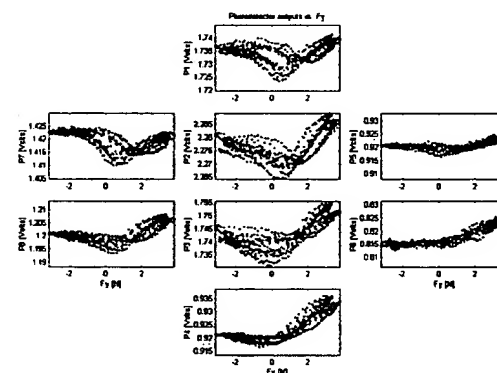Figure 15:   Response to Longitudinal Shear

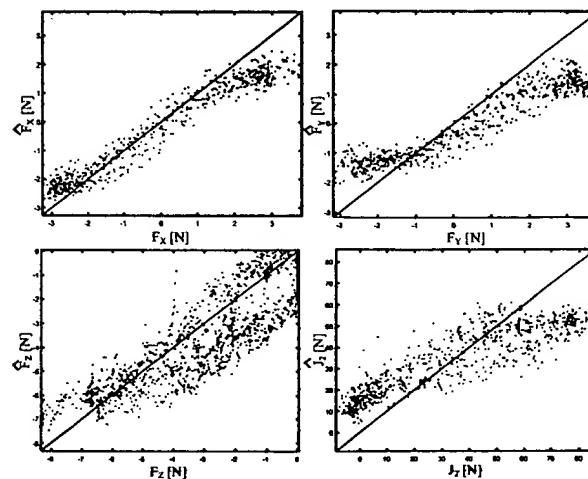Figure 16:   Sensor Output vs. Longitudinal Shear

5.   Analysis

Figure 17:   Predicted vs. Actual Forces/Posture

As seen in section 4, each of the four inputs under consideration results in a unique pattern of photodetector responses. It should therefore be possible to simultaneously estimate the inputs based on the photodetector outputs. As a first step, a multivariate linear least squares regression is performed using data from the four experiments to create a linear model:

$$F = \beta\,(P - P_0) + \varepsilon,$$

where P is an 8x1 vector of photodetector outputs, and F is a 4x1 vector consisting of F_X, F_Y, F_Z, and J_2, β is a 4x8 matrix relating the two, and ε is the residual vector. The photodetector outputs from the four experiments can then be used to generate predicted values of the three forces and bending angle. The results of the regression are shown in Figure 17, where the predicted inputs are plotted vs. the measured inputs for each of the four experiments. The diagonal line passing through each plot represents the ideal one-to-one relationship between actual and predicted inputs. This linear model appears to work well over the dynamic ranges of F_X and F_Z, but not so well for F_Y and J_2, whose predictions are not as centered about the diagonal. This problem must be solved in future work by using a non-linear model to relate inputs and outputs.

6. Conclusion

In this paper, a new method for measuring the posture of human fingers and shear forces at the fingertips has been presented. A wearable fingernail sensor with a 2-dimensional array of photodetectors is capable of measuring the pattern of color change (or change in blood volume) of the fingernail. Experiments were performed to demonstrate the relationships between the photodetector outputs and various inputs including finger joint angle, normal force, lateral shear, and longitudinal shear force. The results show that each input has a unique pattern of response. A multivariate linear regression was used to create a model capable of predicting all four inputs based on the photodetector outputs. Future work will involve more extensive experimentation and design of non-linear models that are capable of predicting finger forces and posture with greater accuracy.

This method will be useful for monitoring human skills and behavior during manipulation, performing teleoperation, and interacting with machines and virtual environments. By measuring shear forces at the human fingertip without placing a sensor underneath the fingertip, it would even be possible to replace a computer mouse with a wearable fingernail sensor. The user could simply push his or her finger against a surface to generate shear forces in two dimensions. Incorporating normal touching force and finger bending could further augment the functionality of such an interface.

References

[1]   D.J. Sturman and D. Zeltzer, "A Survey of Glove-base Input," *IEEE Computer Graphics & Applications*, Vol. 14, No. 1, pp. 30-39, 1994.

[2]   J. Webster, Ed., *Tactile Sensors for Robotics and Medicine*. New York: Wiley, 1988.

[3]   D. Beebe, D. Denton, R. Radwin, J. Webster, "A Silicon-Based Tactile Sensor for Finger-Mounted Applications," *IEEE Trans. on Biomedical Engineering*, Vol. 45, No. 2, pp. 151-159, 1998.

[4]   T. Jensen, R. Radwin, and J. Webster, "A Conductive Polymer Sensor for Measuring External Finger Forces," *J. of Biomechanics*, Vol. 24, No. 9, pp. 851-858, 1991.

[5]   R. Liu, L. Wang, and D. Beebe, "Progress Towards a Smart Skin: Fabrication and Preliminary Testing," *Proc. of the 20th Annual Int. Conf. of the IEEE Engineering in Medicine and Biology Society*, Vol. 20, No. 4, 1998.

[6]   B. McCarragher, "Force Sensing from Human Demonstration Using a Hybrid Dynamical Model and Qualitative Reasoning," *Proc. IEEE Int. Conf. on Robotics and Automation*, Vol. 1, pp. 557-563, 1994.

[7]   S. Sato, M. Shimojo, Y. Seki, A. Takahashi, and S. Shimuzu, "Measuring System for Grasping," *IEEE Int. Workshop on Robot and Human Communication*, pp. 292-297, 1996.

[8]   I. Kim and H. Inooka, "Determination of Grasp Forces for Robot Hands Based on Human Capabilities," *Control Engineering Practice*, Vol. 2, No. 3, pp. 415-420, 1994.

[9]   M. Castro and A. Cliquet, Jr., "A Low-Cost Instrumented Glove for Monitoring Forces During Object Manipulation," *IEEE Trans. on Rehabilitation Engineering*, Vol. 5, No. 2, pp. 140-147, 1997.

[10]   H. Yun, D. Cannon, A. Freivalds, and G. Thomas, "An Instrumented Glove for Grasp Specification in Virtual-Reality-Based Point-and-Direct Telerobotics," *IEEE Trans. on Systems, Man, and Cybernetics*, Part B, Vol. 27, No. 5, pp. 835-846, 1997.

[11]   S. Mascaro and H. Asada, "Hand-in-Glove Human-Machine Interface and Interactive Control: Task Process Modeling Using Petri Nets," *Proc. of the IEEE Int. Conf. on Robotics and Automation*, Vol. 2, pp. 1289-1295, 1998.

[12]   R.D. Howe and M.R. Cutkosky, "Dynamic Tactile Sensing: Perception of Fine Surface Features with Stress Rate Sensing," *IEEE Trans. on Robotics and Automation*, Vol. 9, No. 2, pp. 140-151, 1993.

[13]   J.L. Novak, "Initial Design and Analysis of a Capacitive Sensor for Shear and Normal Force Measurement," *Proc. of the IEEE Int. Conf. on Robotics and Automation*, Vol. 1, pp.137-144, 1989.

[14]   S. Mascaro, and H. Asada, "Fingernail Touch Sensors: Spatially Distributed Measurement and Hemodynamic Modeling," *Proc. of the IEEE Int. Conf. on Robotics and Automation*, 2000.

[15]   A.P. Spence, *Basic Human Anatomy*. Menlo Park, California: Benjamin/Cummings, 1982.

[16]   Y. Nakamura, *Advanced Robotics: Redundancy and Optimization*. Reading, Massachusetts: Addison-Wesley, 1991.